Supplementary Material for "NMR Analysis of a Stress Response Metabolic Signaling Network" by Bo Zhang, Steven Halouska, Charles E. Schiaffo, Marat R. Sadykov, Greg A. Somerville, and Robert Powers

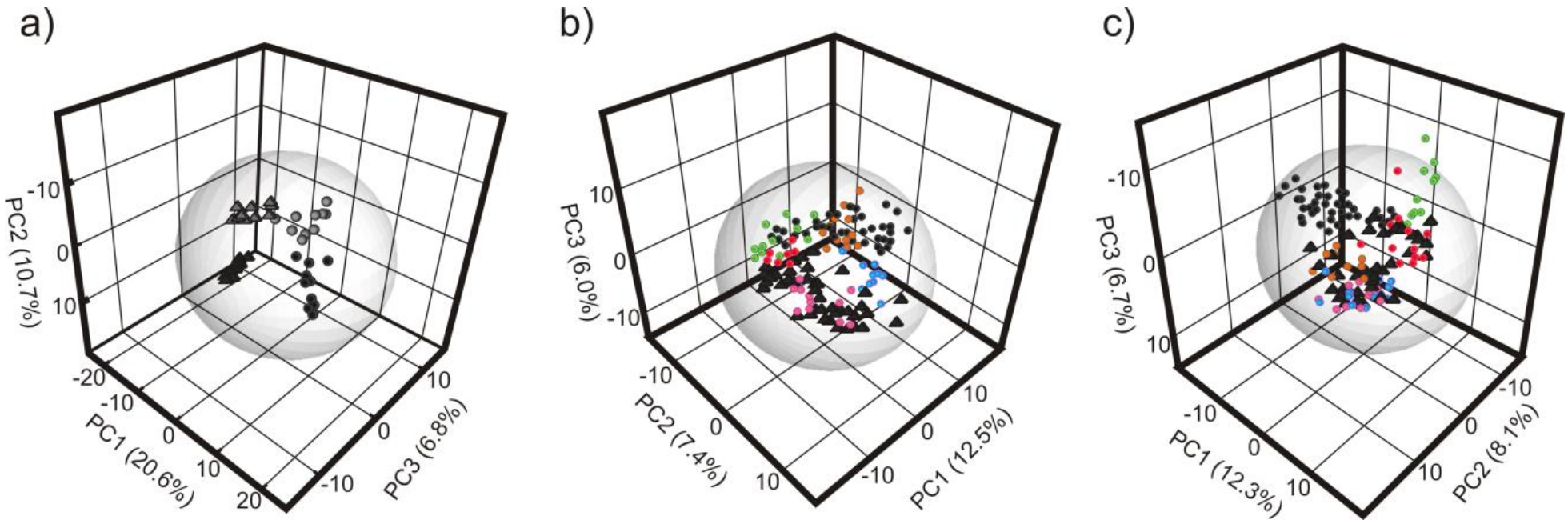

Figure 1S: Three dimensional versions of the 2D PCA scores presented in Figure 2b, Figure 3B, and Figure 4B, respectively. **a**) 3D PCA scores plot comparing *S. epidermis* 1457 strain (circles) and aconitase mutant (triangles) grown for 2 hours (grey) and 6 hours (black). The PCA model consists of 3 significant components where the contribution (R^2) for each successive component is 20.6%, 10.7%, and 6.8%. The overall cross validation (Q^2) is 15.9%, 7.58%, and 2.7%, respectively. **b)** 3D PCA scores plot comparing wild-type *S. epidermidis* 1457 cells grown 6 h in standard TSB media (●), with *S. epidermidis* 1457 cells grown 6 h in iron-depleted media (DTSB) (●), with the addition of 4% ethanol (●),with the addition of 2% glucose (●), with the addition of 0.06 µg/mL tetracycline (●), with the addition of 5% NaCl (●), and 6 h growth of aconitase mutant strain 1457-*acnA*::*tet*M in standard TSB media (▲). The PCA model consists of 5 significant components where the contribution (R^2) for each successive component is 12.5%, 7.5%, 6.0%, 3.8%, and 3.3%. The overall cross validation (Q^2) is 15.9%, 7.58%, and 2.7%, respectively. **c)** 3D PCA scores plot comparing wild-type *S. epidermidis* 1457 cells grown 6 h in standard TSB media (●), 6 h growth of aconitase mutant strain 1457-*acnA*::*tet*M in standard TSB media (▲), aconitase mutant strain 1457-*acnA*::*tet*M in iron-depleted media (DTSB) (●), with the addition of 4% ethanol (●), with the addition of 2% glucose (●), with the addition of 0.06 µg/mL tetracycline (●), and with the addition of 5% NaCl (●). The PCA model consists of 5 significant components where the contribution (R^2) for each successive component is 12.3%, 8.1%, 6.7%, 3.8%, and 3.4%. The overall cross validation (Q^2) is 10.1%, 6.8%, 6.0, 1.6%, and 2.3%, respectively.

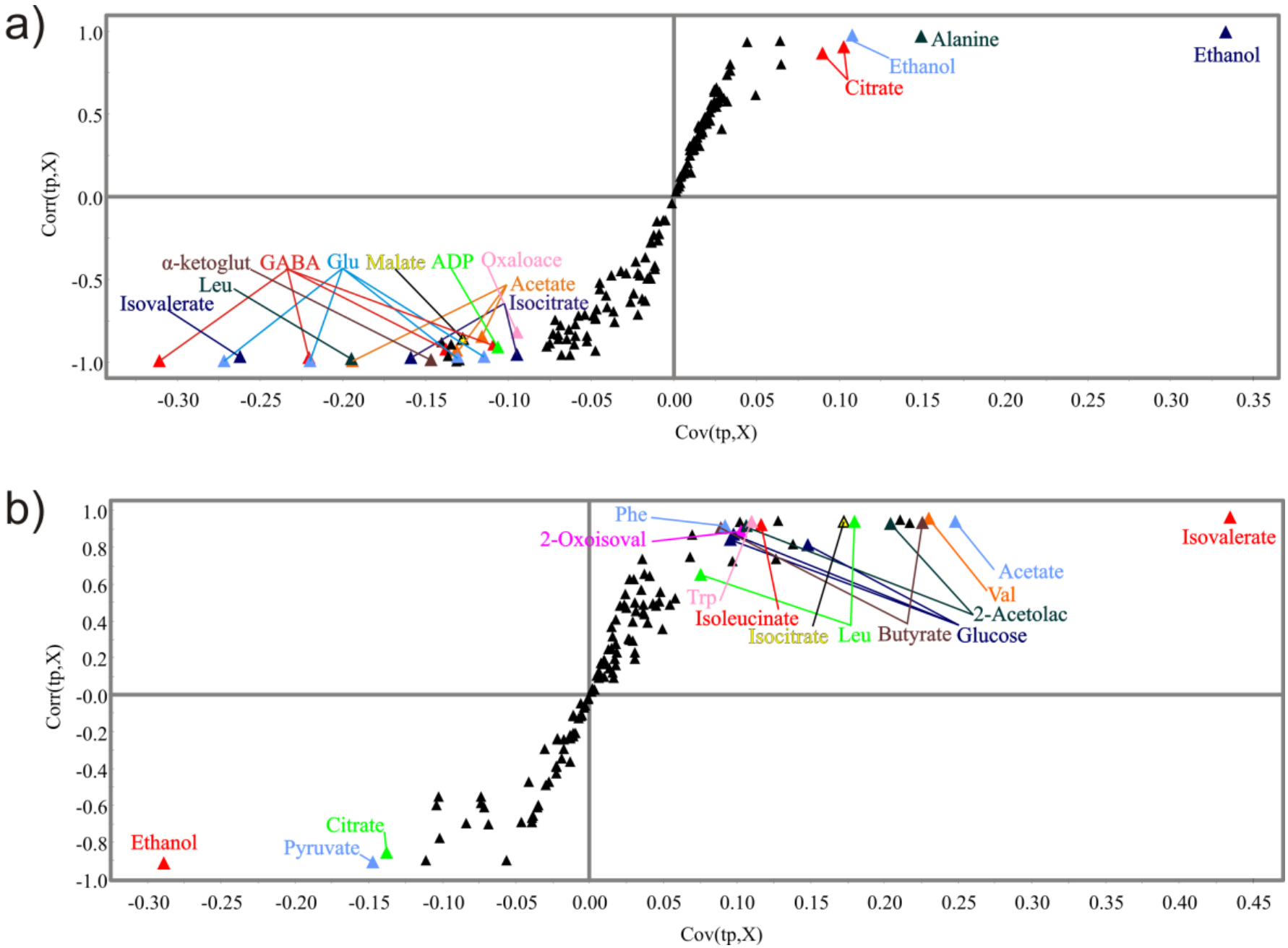
a)
Corr(tp,X)
Cov(tp,X)
Alanine
Ethanol
Citrate
Ethanol
α-ketoglut
GABA
Glu
Malate
ADP
Oxaloace
Acetate
Isocitrate
Leu
Isovalerate
b)
Corr(tp,X)
Cov(tp,X)
Phe
2-Oxoisoval
Isovalerate
Acetate
Val
Trp
Isoleucinate
2-Acetolac
Isocitrate
Leu
Butyrate
Glucose
Ethanol
Citrate
Pyruvate

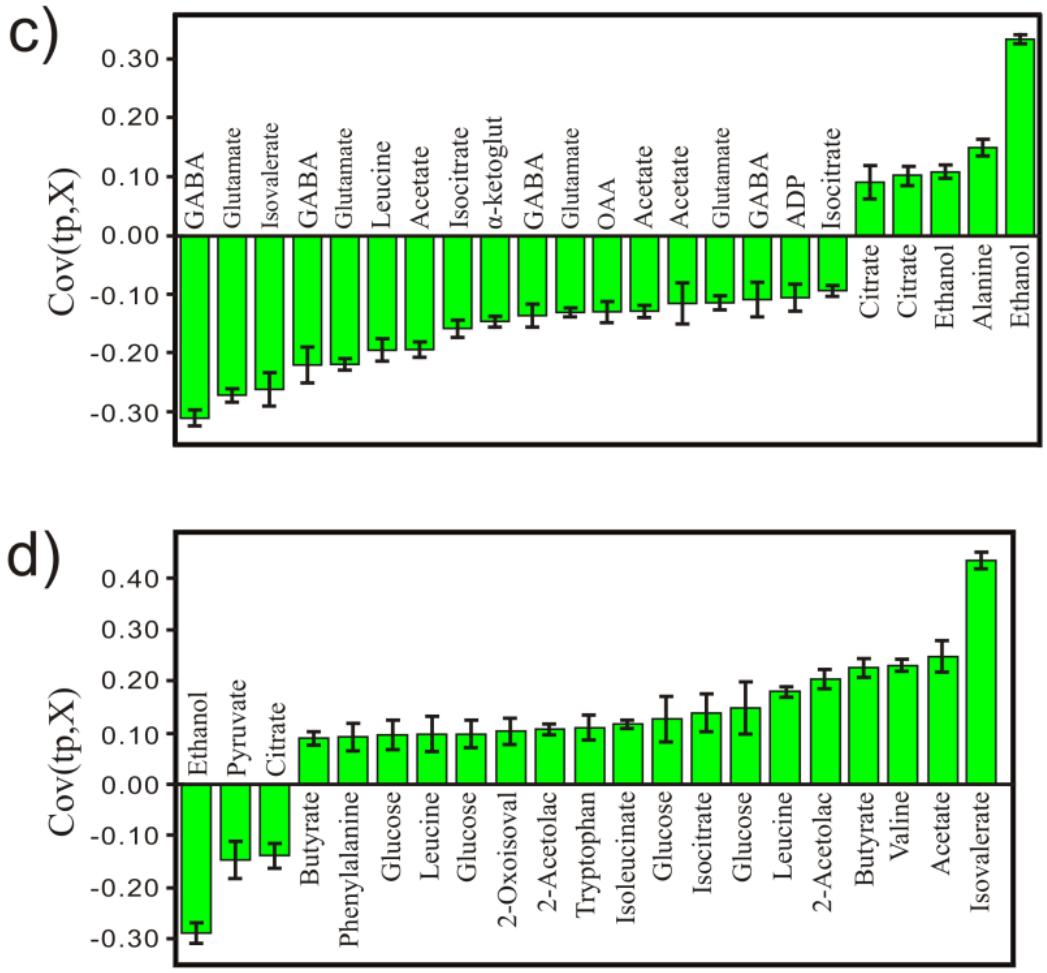

Figure 2S: a) OPLS-DA S-plots comparing the *S. epidermidis* 1457 and aconitase mutant strain 1457-*acnA*::*tet*M where both cell cultures were grown for 6 hours. The two cell cultures were shown be separated along the PC1 axis in Figure 2a. Each point in the S-plot represents a specific bin containing a chemical shift range of 0.025 ppm, where the points at the extreme ends of the S-plot are the major contributors to the class distinction. Each point was identified to a specific metabolite using the Human Metabolomics Database and Madison Metabolomics Database. All the identified metabolites are associated with TCA cycle inactivation. **b)** OPLS-DA S-plot comparing the mutant strain 1457-*acnA*::*tet*M grown for 2 hours and 6 hours. The two conditions are shown to be separated along the PC2 axis in Figure 2a. The metabolites identified are associated with variations in the utilization of glucose for cell growth. **c)** OPLS-DA loading plot comparing *S. epidermidis* 1457 and aconitase mutant strain 1457-*acnA*::*tet*M where both cell cultures were grown for 6 hours. Negative values indicate a decrease in peak intensity when comparing the wild type to the mutant, while positive values indicate an increase in peak intensity. These results are comparable to the bar graphs depicted in figure 6 from the analysis of 2D NMR data. **d)** OPLS-DA loading plot comparing the mutant strain 1457-*acnA*::*tet*M grown for 2 hours and 6 hours.

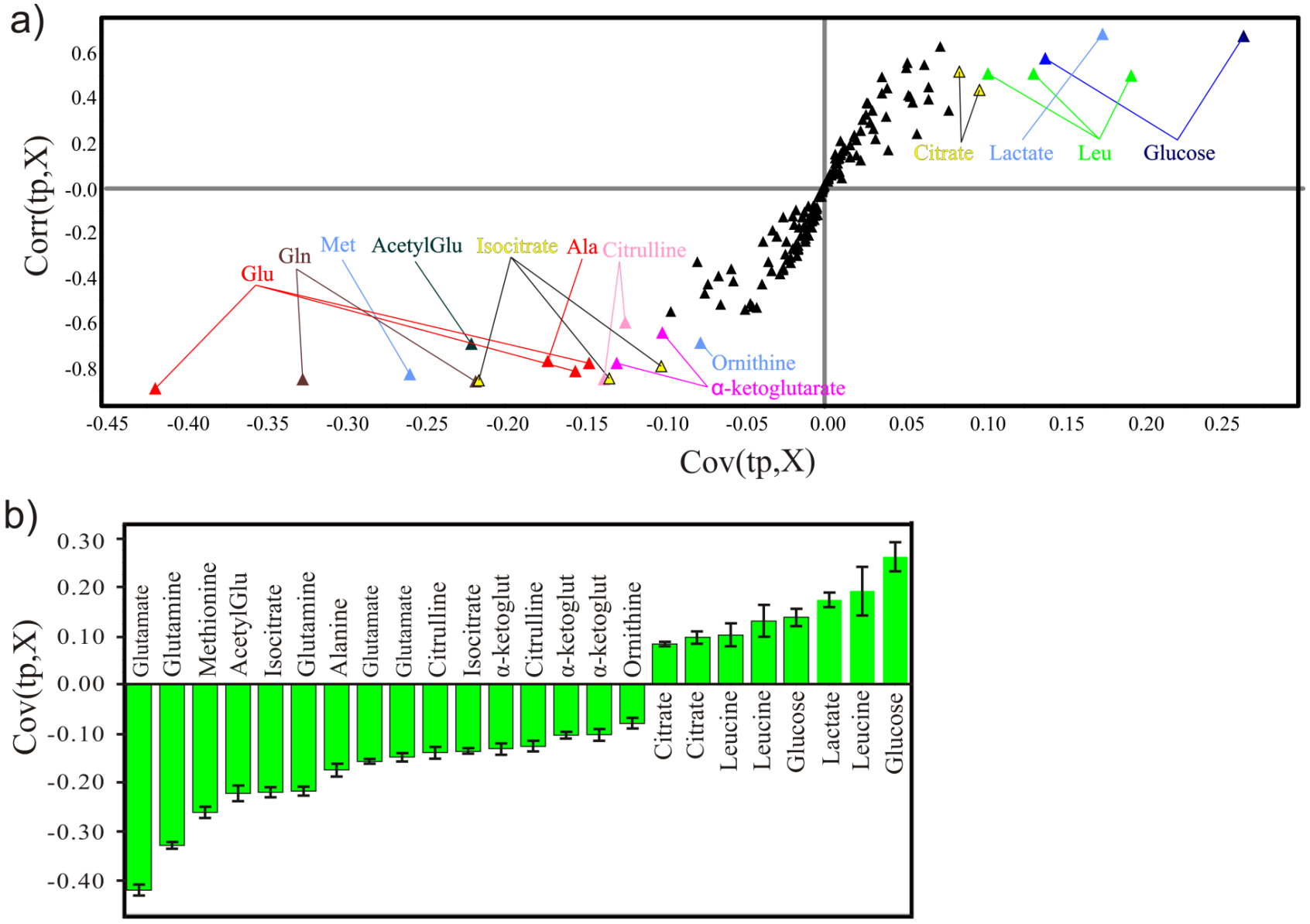

Figure 3S: a) OPLS-DA S-plots comparing wild-type *S. epidermidis* 1457 and *S. epidermidis* cultured under the different stress conditions described in Figure 3. **b)** OPLS-DA loading plot showing the contribution of the identified metabolites from the S-plot. These results are comparable to the bar graphs depicted in figure 6 from the analysis of 2D NMR data.

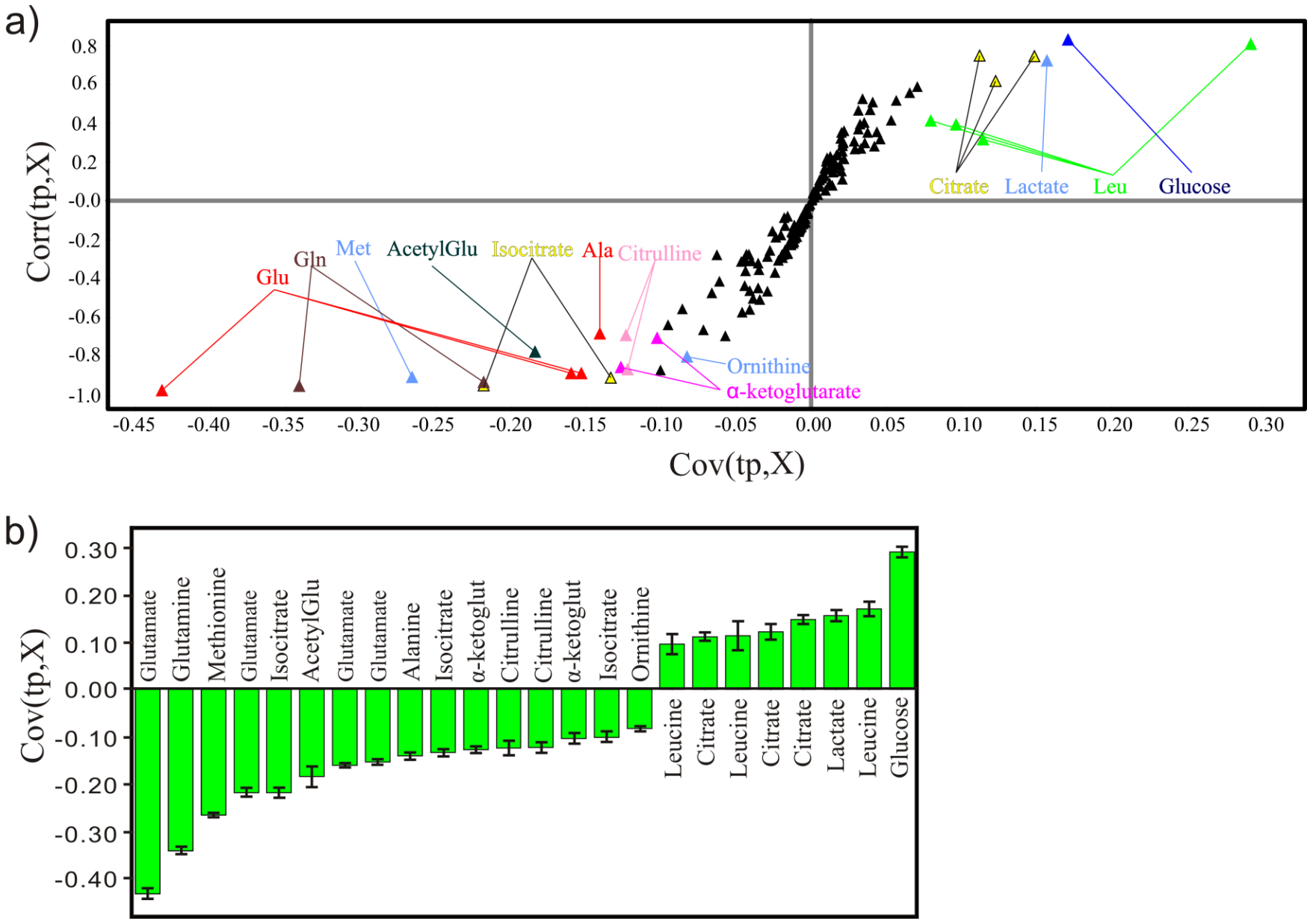

Figure 4S: a) OPLS-DA S-plots comparing the *S.epidermidis* 1457 and the aconitase mutant 1457-*acnA*::*tet*M under the different stress conditions described in Figure 4. **b)** OPLS-DA loading plot showing the contribution of the identified metabolites from the S-plot. These results are comparable to the bar graphs depicted in figure 6 from the analysis of 2D NMR data.

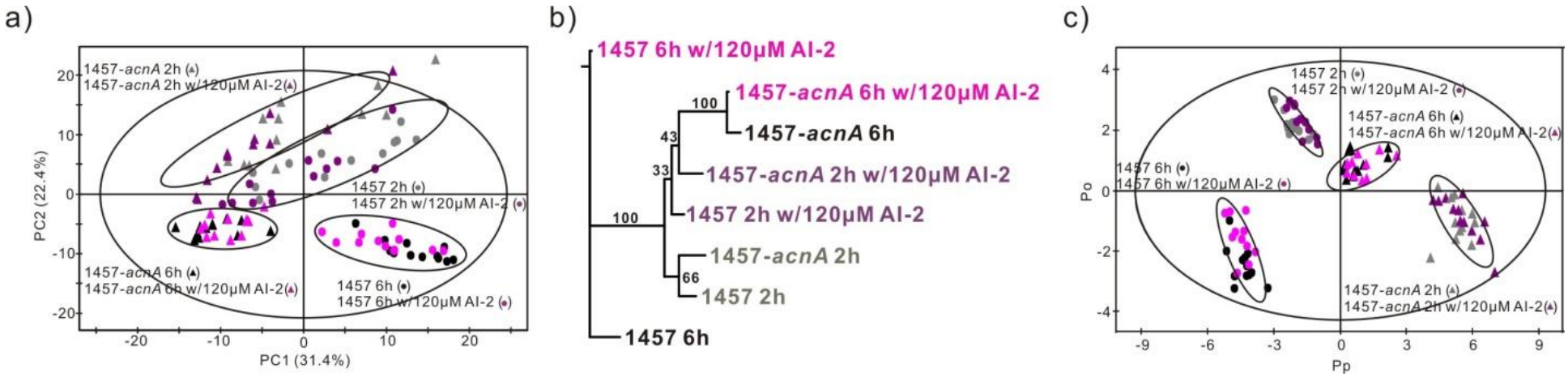

Figure 5S: 2D PCA scores plot comparing wild-type *S. epidermidis* strain 1457 and aconitase mutant strain 1457-*acnA*::*tet*M with and without the addition of 400 nM of AI-2. Cells were grown for 2 h or 6 h in standard TSB media, 2 h growth of wild-type *S. epidermidis* strain 1457 with AI-2 (●) and without AI-2 (●); aconitase mutant strain 1457-*acnA*::*tet*M with AI-2 (▲) and without AI-2 (▲); 6 h growth of wild-type *S. epidermidis* strain 1457 with AI-2 (●) and without AI-2. (●); and aconitase mutant strain 1457-*acnA*::*tet*M with AI-2 (▲) and without AI-2 (▲). b) Metabolomic tree diagram generated from the 2D PCA scores plot depicted in (a). The label colors match the symbol colors from the 2D PCA scores plot. Each node is labeled with the boot-strap number, where a value above 50 indicates a statistically significant separation. **c)** 2D OPLS-DA scores plot comparing wild-type *S. epidermidis* strain 1457 and aconitase mutant strain 1457-*acnA*::*tet*M with and without the addition of 400 nM of AI-2. Each pair of cell cultures treated with and without AI-2 were defined as a separate class for a total of four separate classes. The model consists of 1 predictive component and 3 orthogonal components that yielded an R^2X of 0.774, R^2Y of 0.970, and a Q^2 of 0.954

Effect of autoinducer-2 (AI-2) on the S. epidermidis metabolome. Autoinducer 2 (AI-2) is believed to be an intercellular signaling molecule used in quorum sensing by both gram-negative and gram-positive bacteria.[1] AI-2 minimally represses biofilm formation in *S. epidermidis* where it has been reported that AI-2 indirectly effects the transcription of metabolic genes.[2] This raises the possibility that AI-2 may also function by affecting TCA cycle activity. To investigate the impact of AI-2 on the TCA cycle, bacterial cultures of wild-type *S. epidermidis* and the corresponding aconitase mutant strain were treated with AI-2. Zhao *et al.*[3] recently demonstrated that *S. aureus* cultures supplemented with 390 nM of 4,5-dihydroxy-2,3-pentanedione (DPD), the AI-2 precursor molecule, restored a *luxS* deletion mutant. Thus, 400 nM of AI-2 was used for our NMR metabolomics studies since this concentration of AI-2 was identified as physiologically relevant. The 2D PCA and 2D OPLS-DA scores plots comparing AI-2 treated and untreated bacterial cultures indicates AI-2 did not change the typical clustering pattern (Figures 5S). In other words, the NMR metabolomics data suggests AI-2 does not affect TCA activity or cause a corresponding perturbation in the *S. epidermidis* metabolome. This observation is in contrast to the data reported by Li *et al.*, where AI-2 was shown to effect the transcription of numerous metabolic genes.[2] The apparent discrepancy highlights the benefits of NMR metabolomics, where changes in the metabolome reflect actual changes in protein activity. Conversely, a change in a transcriptional profile does not necessarily correlate with a difference in protein activity.[4]

Supplemental References:

1. Miller, M. B.; Bassler, B. L., Quorum sensing in bacteria. *Annu. Rev. Microbiol.* 2001, 55, 165-199.
2. Li, M.; Villaruz, A. E.; Vadyvaloo, V.; Sturdevant, D. E.; Otto, M., AI-2-dependent gene regulation in Staphylococcus epidermidis. *BMC Microbiol* 2008, 8, 4.
3. Zhao, L.; Xue, T.; Shang, F.; Sun, H.; Sun, B., Staphylococcus aureus AI-2 quorum sensing associates with the KdpDE two-component system to regulate capsular polysaccharide synthesis and virulence. *Infect. Immun.* 2010, 78, (8), 3506-3515.
4. Feder, M. E.; Walser, J. C., The biological limitations of transcriptomics in elucidating stress and stress responses. *J. Evol. Biol.* 2005, 18, (4), 901-910.